Earth's Future

RESEARCH ARTICLE
10.1029/2019EF001174

Regional Differences in Sea Level Rise Between the Mid-Atlantic Bight and the South Atlantic Bight: Is the Gulf Stream to Blame?

Tal Ezer[1]

[1]Center for Coastal Physical Oceanography, Old Dominion University, Norfolk, VA, USA

Key Points:
- A recent shift in the location of a hot spot for accelerated sea level rise along the U.S. East Coast was investigated
- Changes in the Gulf Stream strength and position around 2010 seemed to explain the regional changes in coastal sea level
- Interannual and decadal variations in the Gulf Stream can contribute to temporal and spatial changes in sea level rise rates

Correspondence to:
T. Ezer,
tezer@odu.edu

Citation:
Ezer, T. (2019). Regional differences in sea level rise between the Mid-Atlantic Bight and the South Atlantic Bight: Is the Gulf Stream to blame?. *Earth's Future*, *7*, 771–783. https://doi.org/10.1029/2019EF001174

Received 4 FEB 2019
Accepted 16 MAY 2019
Accepted article online 25 JUN 2019
Published online 13 JUL 2019

Abstract Recent studies appear to show that a "hot spot" for accelerated sea level rise (SLR) shifted around 2010 from the Mid-Atlantic Bight (MAB) to the South Atlantic Bight (SAB) and south Florida. The role of the Gulf Stream (GS) in this shift was thus investigated. The findings show that in the ~15–20 years before, SLR was accelerating in the MAB due to weakening and southward shifting of the GS. After 2010, however, SLR started slowing down in the MAB due to strengthening and northward shifting of the GS. Thermosteric effects seen in altimeter data indicate a warming trend south of 35°N that started around 2010 and contributed to increased SLR south of Cape Hatteras. However, in the MAB, after the GS separated from the coast, the warming of the Subtropical Gyre and cooling of nearshore waters resulted in an opposite SLR response and strengthening of the GS front. Oscillations with periods of 2–5 years dominated the GS flow and coastal sea level variability, but the GS in the MAB is often out of phase with the GS in the SAB due to eddies and recirculation gyres. These oscillations can create temporal changes in SLR rates that are ~10 times larger than the long-term trend, so recent changes in the local "hot spot" may not be interpreted as a sign of a shift in the long-term trend, but more likely a temporal shift associated with interannual and decadal variations in the North Atlantic.

Plain Language Summary Regional changes in sea level rise (SLR) rates along the U.S. East Coast and the role of the Gulf Stream (GS) in those changes are investigated, explaining why the largest SLR rates were found north of Cape Hatteras before 2010 and south of Cape Hatteras after 2010. Before 2010 SLR was accelerating in the MAB due to weakening and southward shifting of the GS, but after 2010 SLR started slowing down in the MAB due to strengthening and northward shifting of the GS. Because of the GS dynamics and its distance to shore, a warming trend south of 35°N that started around 2010 had different sea level response in the north and south. Oscillations with periods of 2–5 years were also investigated.

1. Introduction

Numerous studies of sea level rise (SLR) along the U.S. East Coast show large SLR acceleration between Cape Hatteras in the south and Cape Cod in the north (Boon, 2012; Ezer & Corlett, 2012; Sallenger et al., 2012), which resulted in accelerated coastal flooding in this region (Ezer & Atkinson, 2014; Sweet & Park, 2014). Note that the regional SLR acceleration in those studies was based on long-term tide gauge data collected mostly prior to ~2010. This region of the Mid-Atlantic Bight (MAB) north of Cape Hatteras was thus labeled as a "hot spot" for accelerated SLR, and some studies (e.g., Ezer, 2015; Ezer et al., 2013; Goddard et al., 2015; Sallenger et al., 2012) suggest that the acceleration may be attributed to potential slowdown of the Atlantic Meridional Overturning Circulation (AMOC) (Caesar et al., 2018; McCarthy et al., 2012; Smeed et al., 2013) and its upper branch, the Gulf Stream (GS). However, unlike the hot spot in the MAB region, during the same period only a smaller acceleration, comparable to the global SLR acceleration, was found in the South Atlantic Bight (SAB) (e.g., see Figure 3b in Ezer, 2013). (Hereafter, the SAB coast refers to the region from Key West, Florida, to Cape Hatteras, North Carolina). This spatial difference in SLR trends between the SAB and MAB evoked the idea that ocean dynamics may play a role through the interaction between sea level and GS variabilities (Ezer, 2013, 2015, 2017, 2018; Ezer et al., 2013). In the MAB, after the separation of the GS from the coast at Cape Hatteras, variations in the GS's strength and position increase due to meanders, eddies, and recirculation gyres, while in the SAB, GS variations there (i.e., in the Florida Current, FC) are more limited due to the closeness of the current to the coast. The response on the coast to offshore variations in the GS (Ezer et al., 2013) or winds (Woodworth et al., 2016) may be

different in the SAB and in the MAB. The different topography in the two regions and the sharp coastline change at Cape Hatteras can impact coastal trapped waves (Hughes & Meredith, 2006; Huthnance, 1978) and limit transfer of signals between the MAB and the SAB, as demonstrated by numerical simulations (Ezer, 2016, 2017).

Numerous studies indicate that on a wide range of time scales, from daily changes to interannual and decadal variations, weakening in the GS flow (i.e., decreasing surface geostrophic current associated with sea level slope across the GS) is related to elevated coastal sea level on the onshore side of the current (Ezer, 2015, 2016; Ezer et al., 2013; Ezer et al., 2017; Ezer & Atkinson, 2014, 2017; Goddard et al., 2015; Park & Sweet, 2015; Wdowinski et al., 2016). Combining GS's induced sea level anomalies with long-term SLR trends and land subsidence resulted in an increase in unpredictable minor flooding (so called "sunny day" or "nuisance" flooding) in coastal cities such as Norfolk, VA, or Miami, FL (Ezer & Atkinson, 2014; Park & Sweet, 2015; Wdowinski et al., 2016). While changes in wind patterns and atmospheric pressure can also contribute to coastal sea level variability (Piecuch et al., 2016; Piecuch & Ponte, 2015; Woodworth et al., 2016), the focus here will be on the contribution from variations in the GS. Note, however, that while direct wind- and pressure-driven sea level variations are not considered here, long-term variations in the GS are indeed driven by basin-wide changes in wind, thermal and circulation patterns associated, for example, with El Niño–Southern Oscillation (ENSO), North Atlantic Oscillation (NAO), and AMOC; all those variations will be combined here under the term "low-frequency modes."

The motivation for this investigation comes from several recent studies that appear to challenge the previous findings (summarized above) of accelerated SLR hot spot in the MAB and a lack of acceleration in the SAB. First, Wdowinski et al. (2016) found significant acceleration of SLR in south Florida where SLR rates increased from ~3 mm/year before 2006 to ~9 mm/year for 2006–2014; this change caused significant increase of flooding in Miami. Then, Valle-Levinson et al. (2017) found that SLR south of Cape Hatteras accelerated in 2011–2015, whereas recent SLR rates there increased to over 20 mm/year; the study suggested that cumulative effects of NAO and ENSO variations are responsible for the changing pattern of the hot spot location and timing. Finally, Domingues et al. (2018) found that during 2010–2015 SLR rates in the SAB, south of Cape Hatteras, increased to ~25 mm/year, some 5 times the global rates for this period, while SLR rates recently decreased north of Cape Hatteras. The latter study suggested that the acceleration of sea level in the SAB was caused by unusual warming of the FC, while the deceleration in the MAB was caused by changes in wind and pressure patterns. These recent studies pose several questions that will be investigated here: (1) Is this southward shift of the hot spot of accelerated SLR just a temporary change due to interannual or decadal natural cycles or does it signal a potential shift in long-term trends? (2) Why did the SLR trends in the MAB and SAB change in opposite direction? (Are the two regions affected by different forcing as suggested by Domingues et al., 2018?) (3) What role does the Gulf Stream play? (Can differences in the GS dynamics in the SAB and in the MAB explain the observed differences in sea level?). It is important to study the role of the GS, considering the tight relation between the GS and SLR found in so many studies (see above) and the fact that the GS is the main dynamic connector between the SAB and MAB. It must also be acknowledged that the recent shift in SLR was detected over a relatively short period of time of ~5 years, so any conclusive assessments of potential long-term climatic changes will have to wait for longer records with future observations. The questions above will be investigated by comparisons of coastal and offshore data in both regions.

The study is organized as follows. First, the data sources and analysis are described in section 2, then results are presented in section 3. Finally, a discussion of the mechanism involved and a summary of the results are offered in sections 4 and 5.

2. Data Sources and Analysis

Two tide gauge stations, one in the SAB at Charleston, SC, and one in the MAB at Norfolk, VA, are used (Figure 1); hourly water levels were obtained from NOAA (http://opendap.co-ops.nos.noaa.gov/dods/), and daily values were calculated and analyzed. Numerous studies show very coherent sea level variations within each region, but different patterns in the SAB and in the MAB (e.g., Figure 8 in Ezer & Atkinson, 2017; Figure 1 in Domingues et al., 2018). Therefore, a representative measurement from each region seemed sufficient to demonstrate the coastal response (choosing other stations, not shown, did not make

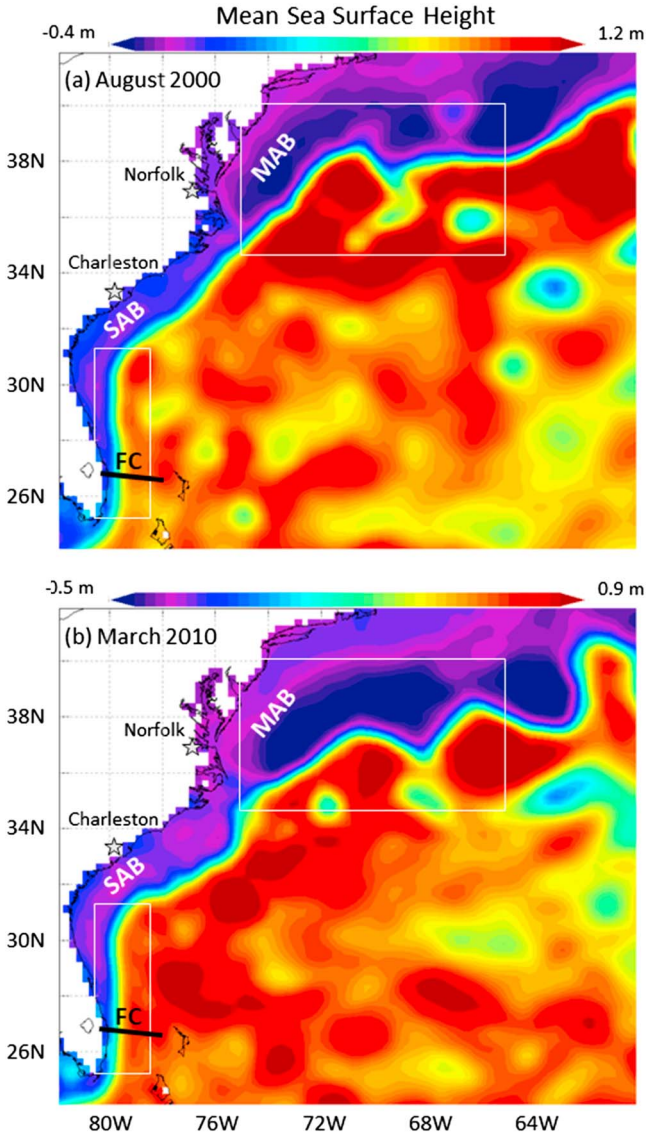

Figure 1. Examples of monthly mean sea surface height from altimeter data for (a) August 2000, when the Gulf Stream (GS) moved farther north, and (b) March 2010, when the GS moved farther south. Two white blocks indicate the two regions where geostrophic velocities are analyzed to represent northward flow of GS-SAB and eastward flow of GS-MAB. Stars represent the two tide gauge stations used, Norfolk, VA, in the Mid-Atlantic Bight (MAB), and Charleston, SC, in the South Atlantic Bight (SAB).

a significant difference in the results). The daily FC transport across the Florida Strait (Baringer & Larsen, 2001; Meinen et al., 2010) was obtained from NOAA's Atlantic Oceanographic and Meteorological Laboratory web (www.aoml.noaa.gov/phod/floridacurrent/). Gridded composed altimeter data based on the AVISO program were obtained from the Copernicus site (http://marine.copernicus.eu/). The altimeter data provided daily sea surface height (SSH) data on 1/4° grid for 1993–2017 (25 years) over the domain in Figure 1, as well as geostrophic velocity in two regions (white boxes in Figure 1). The eastward component of the GS velocity in the MAB (labeled GS-MAB) and the northward component of the GS in the SAB (GS-SAB) are the area mean flow at each box as a function of time; the mean latitude position of the GS in the MAB (PO-MAB) was also calculated from the location of the maximum velocity. While the flow of the GS in the MAB is not exactly eastward (and the flow direction changes with time), analyzing the general onshore/offshore east-west transports and the associated north-south variations in the path of the GS makes the analysis simpler.

To separate variations in the data into different time scales, the Empirical Mode Decomposition (EMD, Huang et al., 1998) analysis method was used. EMD is a nonparametric, nonlinear signal processing tool that has been used in recent years for numerous studies of sea level variability (Chen et al., 2017; Ezer, 2013, 2015; Ezer et al., 2013; Ezer & Corlett, 2012; Kenigson & Han, 2014; Park & Sweet, 2015; Wdowinski et al., 2016). Here, the ensemble EMD (Wu & Huang, 2009) version was used, where an ensemble of simulations with white noise is averaged to provide a more accurate description of low-frequency oscillations compared with a single EMD calculation (nevertheless the term EMD is still used). The EMD separates time series into oscillating modes and a trend, though unlike harmonic analysis or spectral methods, each mode represents oscillations with time-dependent amplitude and frequency. For studying low-frequency oscillations, the EMD is in a way a type of low-pass filter. The analysis can tell us in which modes, for example, variations in sea level are correlated or not with variations in the GS.

3. Results

3.1. Offshore and Onshore SSH

Since only two coastal sea level locations were chosen, it is important to see how well they represent variations in their respective regions. Therefore, correlations were calculated between the closest point to each station in the altimeter data and all other points (Figure 2). High positive correlation within the MAB coast (Figure 2a) and within the SAB coast (Figure 2b) show indeed that sea level variations are coherent within each region, but much smaller correlations are found between points north and south of Cape Hatteras. Sea level near the coast is negatively correlated with offshore SSH along the GS path, this is especially apparent in the SAB where the GS front (Figure 1) separates between positive and negative correlations. This anticorrelation between coastal sea level and the GS strength (represented by the SSH gradient across its path) was discussed in many studies mentioned before (e.g., Ezer et al., 2013; Ezer & Atkinson, 2017; Park & Sweet, 2015).

The thermosteric effect on sea level can be seen from area-averaged SSH north and south of Cape Hatteras (Figures 3a and 3b), which indicates significant differences between the two regions (Figure 3c). The area-averaged SSH of the two regions are calculated when the domain in Figure 1 is divided by the 35°N latitude, so it includes all the open sea east of the coast and west of 60°W. In the northern region (Figure 3a), seasonal

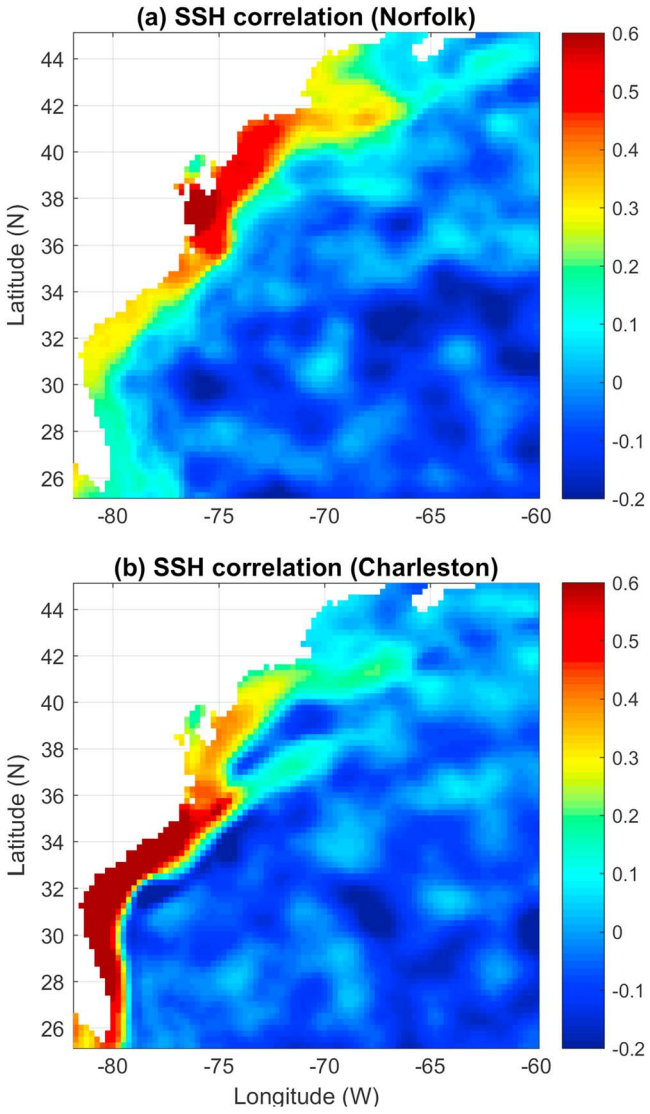

Figure 2. Correlation coefficient of daily sea surface height (SSH) with SSH near (a) Norfolk and (b) Charleston. The annual cycle and long-term trend were removed. Correlations with absolute value greater than ~0.05 have *P* value less than 0.001 (i.e., statistical significance > 99.9%).

variations are larger (consistent with the seasonal cycle of temperature), but interannual variations are smaller when compared with the southern region (Figure 3b). Thermal and wind variations over the Subtropical Gyre may be responsible for the interannual and decadal variations in the south. During those 25 years, warming of the ocean can be seen especially in recent years as steric SSH rises. However, while in the north a gradual warming is seen since circa 2005 (Figure 3a), in the south a large warming trend is seen since circa 2010. The difference in SSH (Figure 3c) shows the recent shift from a period of (relatively) higher SSH in the north (2009–2013) to a period of (relatively) higher SSH in the south (2014–2017). These results are consistent with the findings of Domingues et al. (2018) who showed that between 2015 to 2017 temperature in the Florida Strait shifted from about −1 °C cold anomaly to about +1 °C warm anomaly. Figure 3, however, indicates that this warming trend is part of a large-scale trend over the Subtropical Gyre and not limited to just the Florida Strait. Oscillations with periods of 2–5 years clearly impact the trends as seen from the low-pass filtered records (heavy black lines in Figure 3; these lines were obtained from the low-frequency EMD modes, as discussed later). These oscillations are different in phase and amplitude for the northern and southern regions, thus pointing to different dynamic regional forcing as suggested before (Domingues et al., 2018; Valle-Levinson et al., 2017; Woodworth et al., 2016). Therefore, these oscillations will be further investigated later with the help of the EMD analysis.

3.2. Variability of the Gulf Stream's Flow and Position and Their Relation to Coastal Sea Level

The daily and low-pass filtered records of the two coastal sea level records (Norfolk and Charleston) and the two GS flow regions (GS-MAB and GS-SAB) are shown in Figure 4. Besides the annual cycle, there are clear interannual and decadal variations (order of ~0.1 m in sea level and ~0.5 m/s in GS velocity) that change the temporal trends. It appears as if these variations in the GS-SAB and GS-MAB are out of phase; for example, between 1998 and 2001 the GS-SAB changed from a strong current (mean velocity over 1.6 m/s) to a relatively weak current (mean velocity ~0.7 m/s), while the GS-MAB strengthened at the same time. The upward trend of the GS-MAB flow after 2010 (Figure 4c) and its variations resemble the warming trend seen in SSH in the SAB (Figure 3b), but there is no significant increase in the GS-SAB flow during this period. At other periods, the GS trend in both regions is similar; for example, during the peak warming around 2003–2004 (Figure 3b) the GS was stronger in both regions. Possible dynamic explanation for the change in trend after 2010 is that warming of the Subtropical Gyre increased the temperature gradients across the GS in the MAB, which then strengthen the geostrophic flow. Long-term SLR trends and especially acceleration must be obtained from long records, usually of at least 60 years (Boon, 2012; Ezer & Corlett, 2012; Kenigson & Han, 2014), otherwise decadal and multidecadal variations can contaminate the trends. To demonstrate the contribution of interannual variations to changing trends, the instantaneous changes of sea level and GS flow are shown in Figure 5. The trends were obtained from the daily low-pass filtered records in Figure 4, by calculating the change from day to day (however, the values were converted to change per year to allow comparisons with long-term values, for example, sea level rise in millimeter per year). The variations in SLR trends (Figures 5a and 5b) are ~10 times larger than the mean trend over the 25-year period (standard deviation of ~70 mm/year over mean of 5–7 mm/year), and during short periods SLR can be as large as ±100 mm/year. Therefore, the extremely large SLR of 10–25 mm/year reported for south Florida around 2010–2015 (Domingues et al., 2018; Valle-Levinson et al., 2017; Wdowinski et al., 2016) is not too unusual compared with past

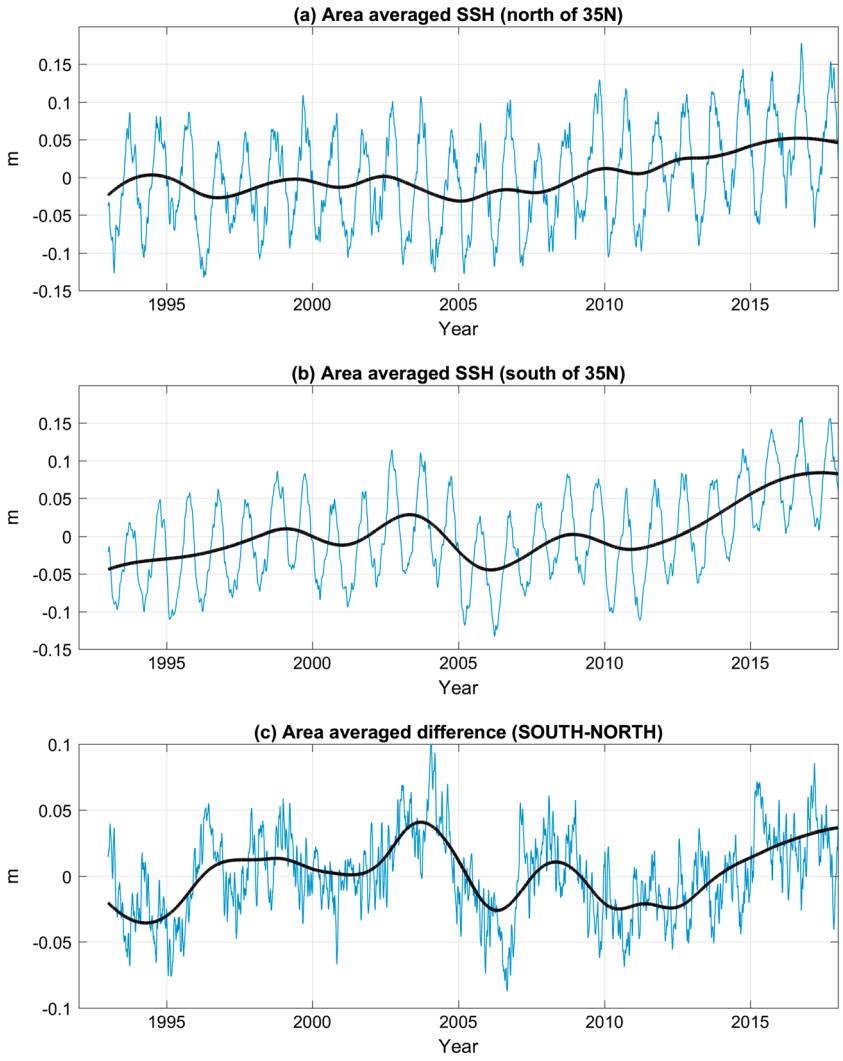

Figure 3. Area mean sea surface height (SSH) calculated for (a) the region north of 35°N in Figure 1, (b) the region south of 35°N, and (c) the difference between (a) and (b). Blue lines are the daily values and black heavy lines are the low-frequency EMD modes (see text).

decadal variations. The daily changes in the GS flow show variability (order ± 0.2 m·s^{-1}·year^{-1}) with oscillations of 2- to 5-year period.

Many studies found connections between the GS position and strength (e.g., Joyce et al., 2000), showing, for example, that during periods of low NAO index the GS tends to shift southward and this shift may be associated with increased coastal sea level in the MAB (Ezer, 2015; Ezer et al., 2013). Figure 6 shows the average strength and north-south position in the MAB region of Figure 1; variations of ~300 km in the GS position are not unusual. Figure 7a shows the distribution of the GS position versus the GS-MAB flow. While there is a statistically significant correlation between a northward GS position and a stronger mean flow, another result is the fact that the variability in the GS position is large when the GS is weak ($\pm 1.5°$ latitude shift for GS-MAB when its velocity is 0.4–0.6 m/s) and the variability is small when the GS is strong ($\pm 0.5°$ latitude shift for GS-MAB when its velocity is 1–1.3 m/s). This may have some implications for predictability and climate change, if the GS will slow down under warmer climate, as suggested by climate models. As for the GS in the SAB, variations in its east-west position are extremely small (not shown) due to the closeness of the FC to the coast; however, variations in the GS-SAB strength are large, as much as ~0.5 m/s (Figure 4d). The variability of the GS-SAB flow results from two components, the inflow of the FC through the Florida Strait and variations due to local wind and mesoscale variability.

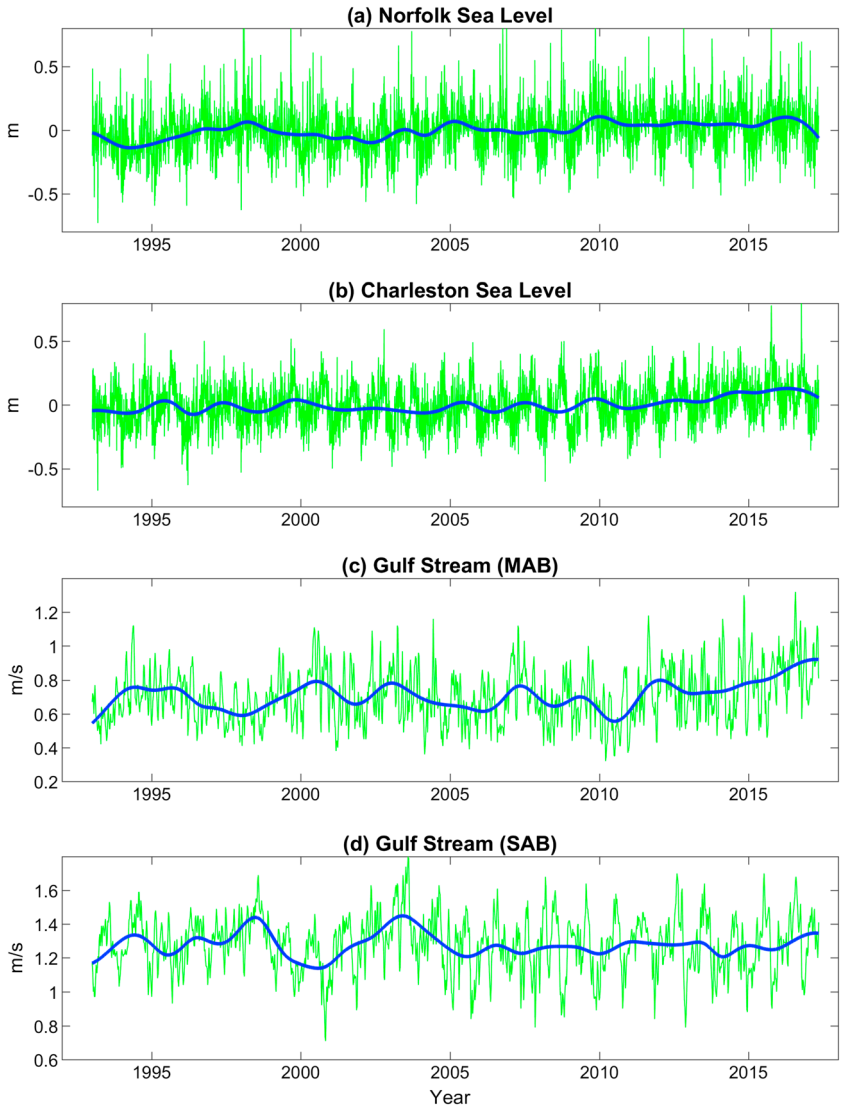

Figure 4. Sea level at (a) Norfolk and (b) Charleston and GS mean flow in (c) MAB and (d) SAB; see Figure 1 for locations. Daily values are in green and low-frequency EMD modes are heavy blue lines; the latter is the sum of the low-frequency Empirical Mode Decomposition modes 9–14 representing oscillations with periods longer than the annual cycle.

Figure 7b shows the distribution of the GS-SAB daily velocity (~25–32°N) versus the FC cable measurements (at ~27°N). As expected, the correlation between the two is positive and significant (statistical significance level over 99.9%), but nevertheless, ~75% of the variability may be driven by local processes within the SAB. For each GS-SAB mean flow value, variations in the FC can vary from the mean by about ±5 Sv (1 Sv = 10^6 m^3/s).

3.3. EMD Analysis of Interannual and Decadal Oscillations

The EMD analysis (actually ensemble EMD, see section 1) for this 25-year-long daily data produces 14 modes (the number of EMD modes is determined by the code and depends on the record length and variability). The modes are defined here as follows: mode 1 is the original data without filtering, modes 2–7 represent high-frequency oscillations with periods of days to months, mode 8 seems to capture the annual cycle, modes 9–13 represent low-frequency oscillations (periods of 2 years and longer) and mode 14 is the long-term trend. The low-pass filtered records in Figure 4 are the sum of modes 9–14 (notes that the sum of modes 2–14 is

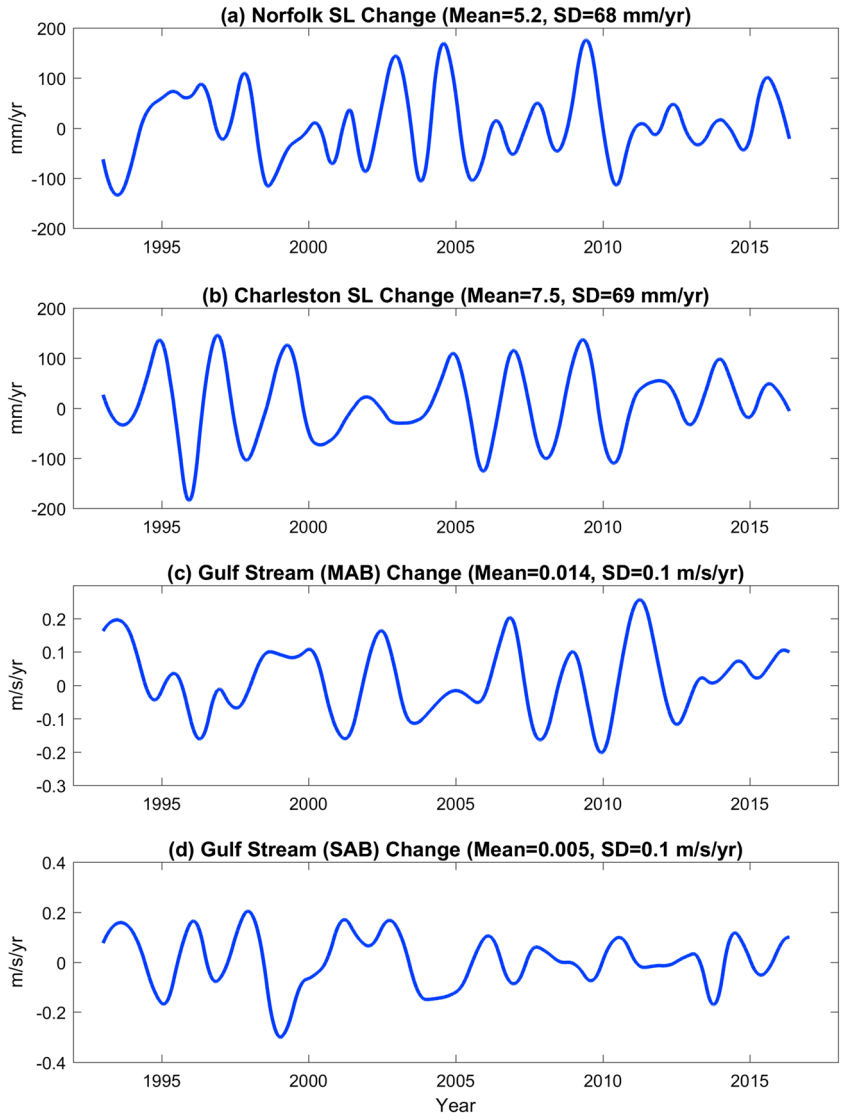

Figure 5. The instantaneous change (local slope) in the low-frequency modes in Figure 4; units were converted from daily change to change per year: (a) and (b) are in units of millimeter per year and (c) and (d) are in units of meters per second per year. To minimize problems with EMD end-effect the last year of the time series is not shown. Note that the standard deviation is ~10 times larger than the mean, indicating that the interannual and decadal variations dominate over the long-term trend. SL = sea level; MAB = Mid-Atlantic Bight; SAB = South Atlantic Bight.

equal to the original data in mode 1). The focus here is on low-frequency modes that show clear oscillations, since these modes can create temporal changes in trends (e.g., Figure 5). Figure 8 compares the GS position (in the MAB) with the GS velocity in the MAB and SAB. Modes 10 and 11 of the GS position (PO-MAB) positively correlated with the GS-MAB velocity but negatively correlated with GS-SAB (Figure 8a represents oscillations with periods of 2–5 years). Therefore, when the GS moves farther north, the GS velocity in the MAB is generally stronger, but the GS in the SAB is weaker—this could result in coastal sea level increase in the south and decrease in the north, as recently reported (Domingues et al., 2018). However, on longer time scales (Figure 8b, modes 12 and 13), the pattern is very different, and all three records are highly correlated with each other (R = 0.95–0.98). This long-period oscillation resembles the large-scale oscillation of the mid-ocean transport of AMOC, which also shows minima around 2010 (see Figure 8 in Ezer, 2015). Therefore, around 2010 there was a change in the GS from southward to northward shifting of its position and from weakening to strengthening currents in both locations. This

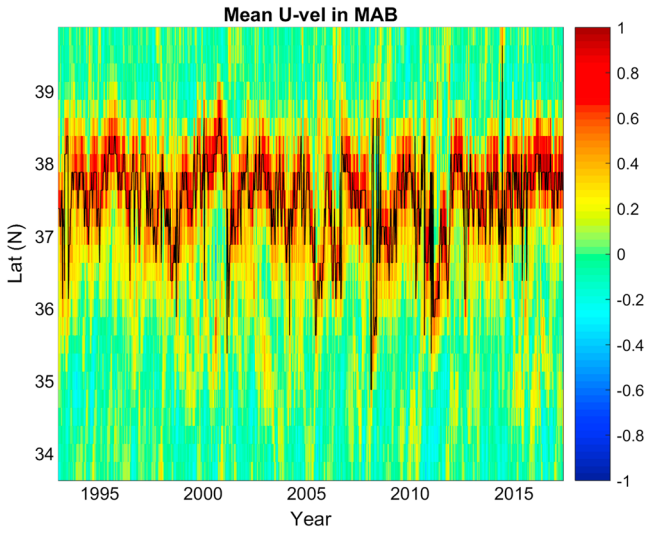

Figure 6. Eastward surface geostrophic velocity component (obtained from AVISO) as a function of time and latitude averaged over the longitudes in the MAB box of Figure 1. MAB = Mid-Atlantic Bight.

result is consistent with several studies that found that during 2009–2010 the NAO index was very low, AMOC was unusually weak and sea level was unusually high along the coast of the MAB (Ezer, 2015; Goddard et al., 2015; McCarthy et al., 2012).

The relation between the two coastal sea level records and the two GS flow records for low-frequency modes is shown in Figure 9. The focus is on modes that show clear oscillations with time scales of multidecadal (Figure 9a), 5–10 years (Figure 9b), and 2–5 years (Figure 9c). The multidecadal GS-MAB and GS-SAB flow modes in Figure 9a are the same as that in Figure 8b, and both are in phase with the GS position trend, as discussed before. However, the coastal sea level in Norfolk and Charleston are ~10 years out of phase with each other, so that coastal sea level in the SAB is positively correlated with the GS flow (R = 0.8 and 0.94), while coastal sea level in the MAB is negatively correlated with the GS flow (R = −0.78 and −0.9; similar to earlier findings of Ezer et al., 2013). The contribution of this multidecadal mode (apparent period of 20–30 years) can result in increased SLR in the south after ~2009 and decreased SLR in the north after circa 2012. An estimate of this contribution shows that at Charleston this mode alone can add ~5 mm/year to the

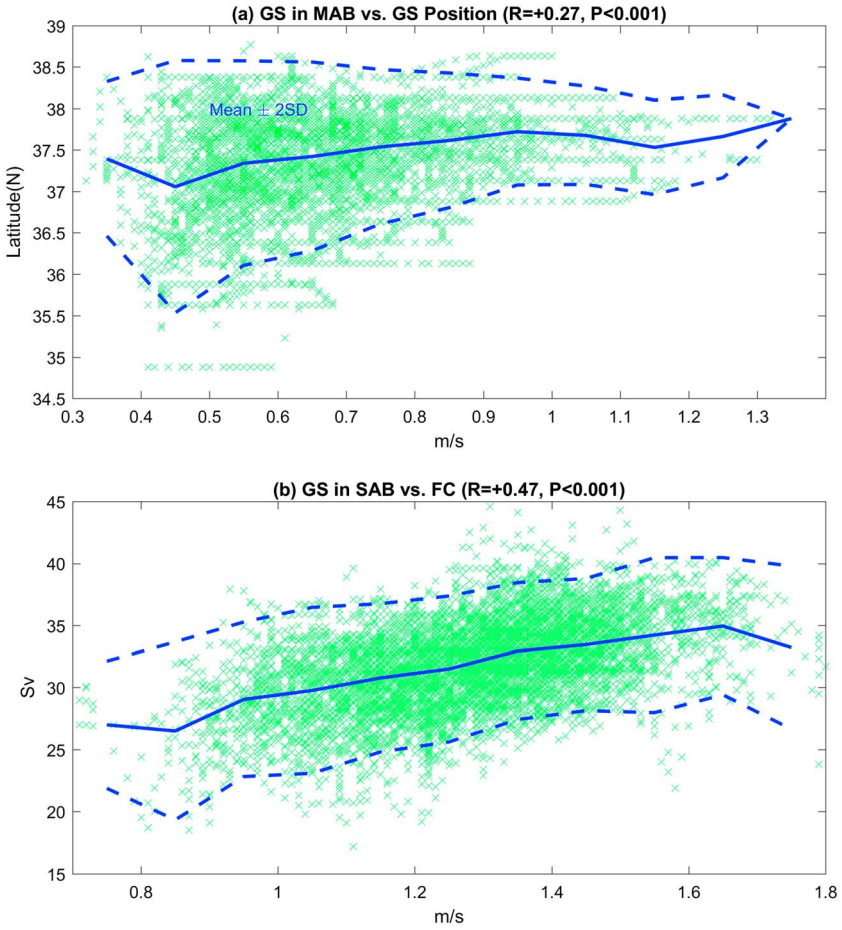

Figure 7. (a) Distribution of daily Gulf Stream (GS) position in MAB versus mean eastward GS velocity in MAB. (b) Distribution of daily transport of the Florida Current (FC; ~27°N) versus mean northward GS flow in the SAB (25–32°N). Mean and 2 standard deviation lines are shown in blue; they were calculated for each 0.1-m/s bin of the x axis. Correlation coefficient, R, and p value are indicated for each panel. MAB = Mid-Atlantic Bight; SAB = South Atlantic Bight.

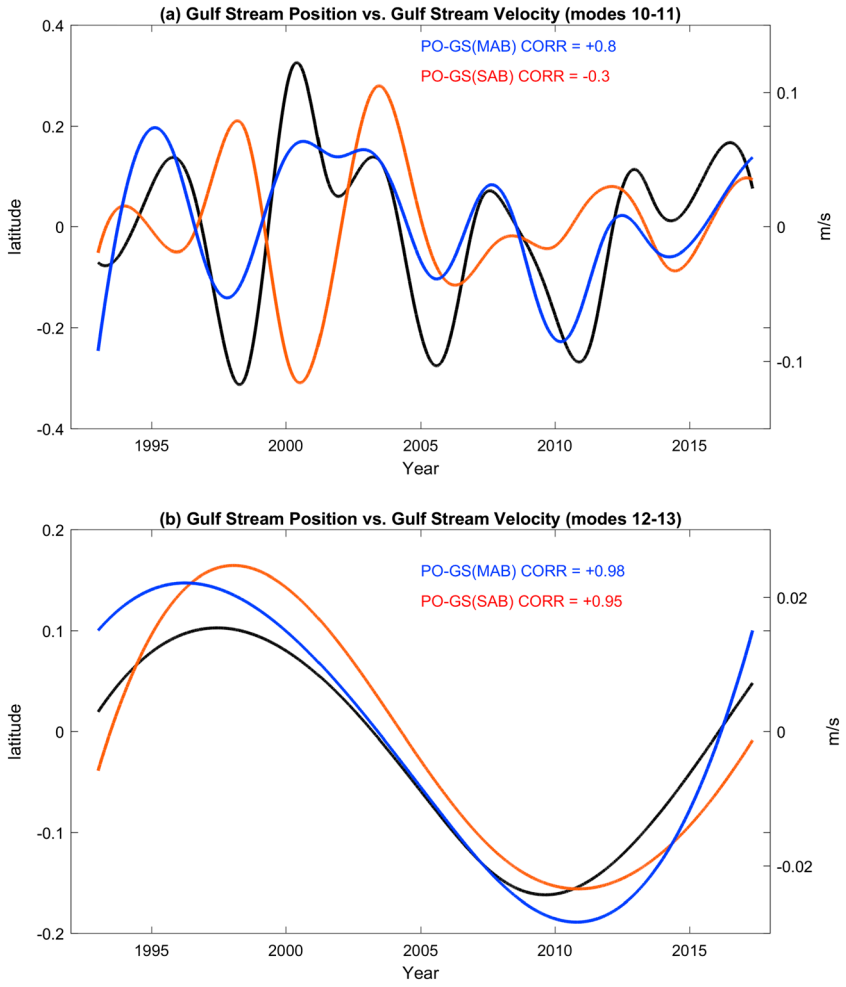

Figure 8. Low-frequency oscillations of the Gulf Stream (GS) position (PO in black; *y* axis on left) in the MAB versus GS velocity (GS-MAB in blue and GS-SAB in red; *y* axis on right). (a) EMD modes 10–11 and (b) EMD modes 12–13 (the lowest-frequency modes, excluding the trend). Correlation coefficients are indicated (all at p values < 0.001). MAB = Mid-Atlantic Bight; SAB = South Atlantic Bight; EMD = Empirical Mode Decomposition.

SLR trend between 2010 and 2015, not an insignificant number compared with the global SLR rate of ~3 mm/year. In contrast to the multidecadal modes where the GS-MAB and GS-SAB are highly coherent with each other ($R = 0.92$), at shorter time scales (5- to 10-year periods; Figure 9b) the two GS currents are anticorrelated with each other ($R = -0.25$ at over 99% confidence level). For those modes, coastal sea levels in both locations are anticorrelated with the nearby GS ($R = -0.78$ for the MAB and $R = -0.58$ for the SAB). This relation is consistent with changes in the slope across the GS as found in previous studies (e.g., Ezer & Atkinson, 2017). At even shorter time scales of interannual variations (periods of 2–5 years, Figure 9c) sea level in Norfolk is not significantly correlated with the GS-MAB, indicating that at these time scales variations in the GS are affected by local variations in wind pattern, recirculation gyres, and mesoscale eddies, rather than by large-scale circulation patterns as the low-frequency modes do. In the SAB on the other hand, the coastal sea level is highly correlated with the nearby GS ($R = -0.67$), which can be explained by the fact that the FC is not too far from the coast, so changes in flow intensity is related to the sea level slope across the GS and thus to coastal sea level.

4. Discussion

The study was motivated by recent observations (Domingues et al., 2018; Valle-Levinson et al., 2017; Wdowinski et al., 2016) that challenged previous perceptions of a “hot spot” of accelerated coastal sea

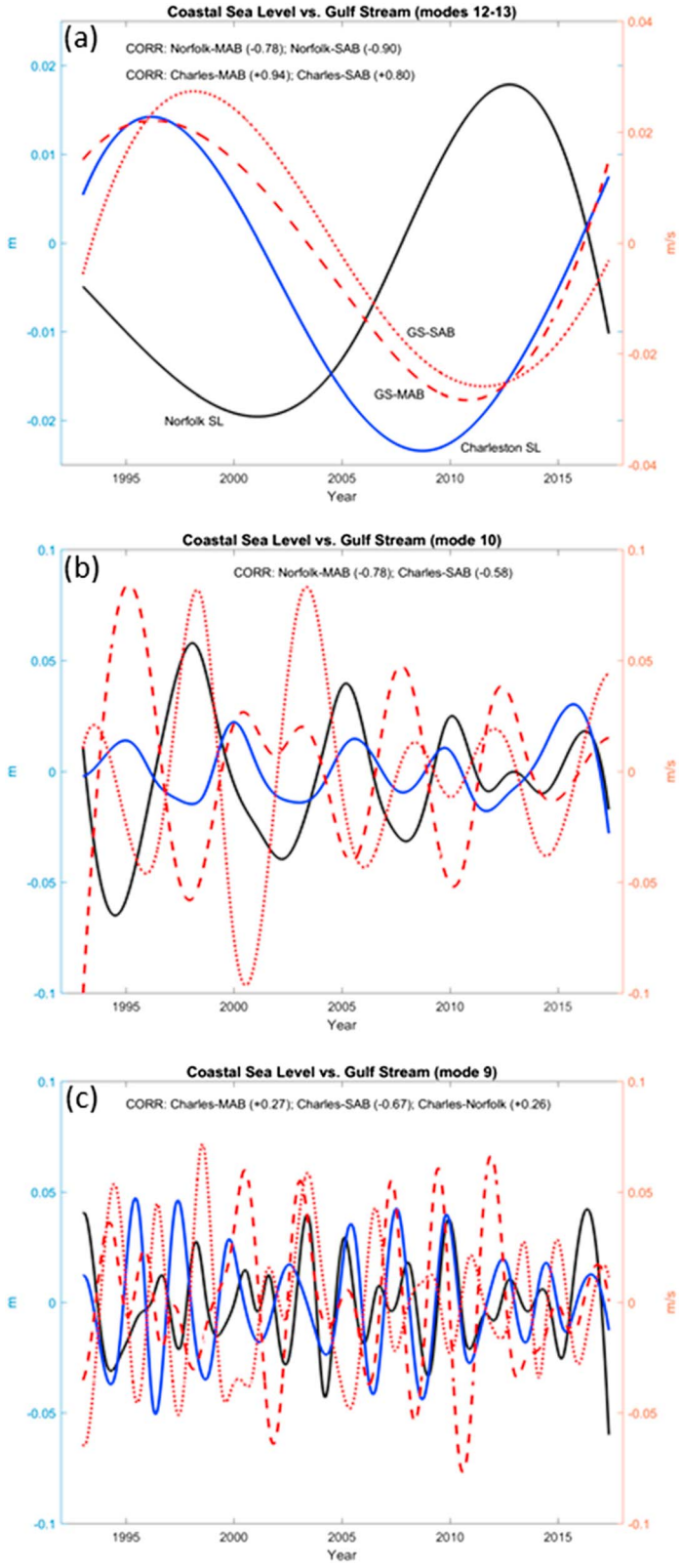

Figure 9. Comparisons between coastal sea level (SL; solid black line for Norfolk and blue for Charleston; *y* axis on left) and Gulf Stream (GS) flow (dash red line for GS-MAB and dotted red line for GS-SAB). (a) EMD modes 12–13, (b) EMD mode 10, and (c) EMD mode 9. Correlation coefficients that are most statistically significant are indicated. MAB = Mid-Atlantic Bight; SAB = South Atlantic Bight; EMD = Empirical Mode Decomposition.

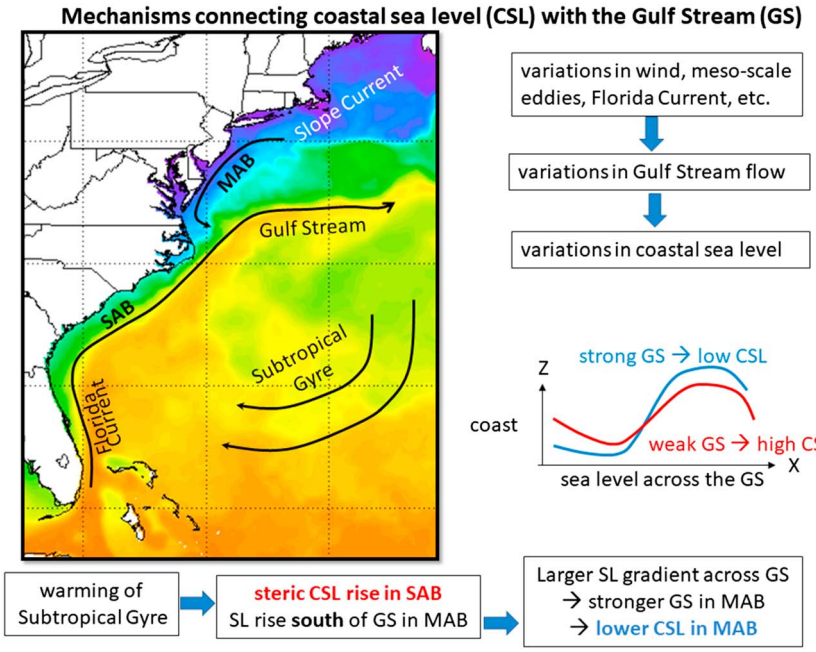

Figure 10. Example of sea surface temperature in the study area (warm to cold temperatures are represented by red to blue colors) and schematics of possible mechanisms that connect variations in the Gulf Stream strength with variations in coastal sea level. The two mechanisms are variations driven by local forcing such as wind (on the right) and variations in temperatures of the Subtropical Gyre (on the bottom). MAB = Mid-Atlantic Bight; SAB = South Atlantic Bight.

level rise north of Cape Hatteras (Boon, 2012; Ezer, 2013; Ezer et al., 2013; Ezer & Corlett, 2012; Goddard et al., 2015; Sallenger et al., 2012; Yin & Goddard, 2013). The earlier studies suggested that the regional SLR acceleration is related to potential slowdown of the GS flow and AMOC. The fact that most of the acceleration was observed north of the point where the GS separates from the coast suggests a role for the GS variability and the recirculation between the GS and the coast. Studies show, for example, that when the GS weakens and/or shifts southward, the southward flow of the Slope Current along the coast of the MAB intensifies and coastal sea level rises (Ezer, 2015; Ezer et al., 2013). Since climate models indicate a potential slowdown of AMOC under a warmer future climate (e.g., Caesar et al., 2018), climatic changes in ocean circulation may have important implications for regional sea level rise and mitigation and adaptation efforts to battle increased flooding in low-laying coasts and cities (Ezer & Atkinson, 2014; Sweet & Park, 2014). The studies that showed large acceleration of SLR in the MAB (compared with the global acceleration) were mostly based on tide gauge data collected before circa 2011 (1969–2011 in Boon, 2012; 1905–2011 in Ezer & Corlett, 2012; 1950–2009 in Sallenger et al., 2012). These studies also showed smaller acceleration in the SAB relative to the MAB during the same period. The high anticorrelations found between the GS flow and SLR along the MAB coast demonstrated the impact of the GS on the coast (e.g., Figure 10 in Ezer et al., 2013). However, more recent measurements, mostly after 2010, now show extremely high SLR rates (~10–25 mm/s) in south Florida and the SAB region, suggesting that the hot spot has flipped from the MAB to the SAB (Domingues et al., 2018; Valle-Levinson et al., 2017; Wdowinski et al., 2016). While Vale-Levinson et al. suggested that these changes are related to cumulative impacts from NAO and ENSO variations, Domingues et al. suggested that warming of the FC causes the increased SLR there, while changes in air pressure and wind contributed to a slowdown of SLR in the MAB. In any case, it is not clear if these recent regional changes are part of a temporary change due to interannual and decadal oscillations or a signal of some long-term shift. This question was investigated here to better understand the mechanisms involved, as illustrated in Figure 10. It is suggested that in addition to the direct GS-coastal sea level relation that results in anticorrelation between the GS strength and sea level rise (Ezer, 2016; Ezer & Atkinson, 2017), there is another mechanism associated with warming of the Subtropical Gyre that can result in opposing coastal sea level response between the SAB and the MAB. The latter process is due to the different proximity of the GS to the coast—in the SAB

where the GS is close to the coast, a warmer GS increases steric sea level, but in the MAB after the GS separated from the coast, a warmer GS and cooler coast waters (Domingues et al., 2018) will strengthen the GS front and reduce costal sea level in the MAB (consistent with the anticorrelation between the GS and coastal sea level, mentioned before).

5. Summary and Conclusions

The major findings here are summarized in the following.

1. The results support the finding of Domigues et al. (2018) that a warmer FC (i.e., GS-SAB) in recent years increased steric sea level south of Cape Hatteras. However, the warming seemed to expand beyond the coast, covering the area south of 35°N and west of 60°W. Fast warming trend in the SAB started after ~2010, while the region north of Cape Hatteras experienced more gradual warming trend since ~2005 (Figure 3). The coastal sea level response after 2010 is consistent with the mechanism describe in Figure 10.
2. The increase in the strength of the GS in the MAB after 2010 (Figure 4) after several years of downward trend can explain the recent slowing down of sea level rise north of Cape Hatteras and is consistent with previous relations between the GS and coastal sea level (e.g., Ezer et al., 2013). Additional contributions from changing atmospheric pressure, wind patterns, or NAO (Domigues et al., 2018; Piecuch & Ponte, 2015; Piecuch et al., 2016; Valle-Levinson et al., 2017; Woodworth et al., 2016) are not excluded, though these processes have not been studied here. Also, the impact of potential long-term slowdown of AMOC on coastal sea level was not addressed here.
3. Interannual and decadal oscillations can create temporal SLR rates that are at least 10 times larger than the long-term rates (Figure 5). Therefore, the unusually high SLR (5 times the global rate) reported in south Florida for 2010–2015 is not unprecedented or an indication of a long-term climatic shift in the "hot spot." Nevertheless, these temporal changes can have significant consequences for increased flooding for several years in places like Miami (Wdowinski et al., 2016). A similar period of unusually high coastal sea level and increased flooding along the U.S. coasts occurred, for example, in 2009–2010, during a period when the AMOC transport dropped by 30% and the NAO index was especially low (Ezer, 2015; Goddard et al., 2015; McCarthy et al., 2012). Abrupt changes in ocean circulation and coastal sea level also happened, for example, in the 1950s and 1970s (Ezer, 2015), but these oscillations are separated from the long-term climate change trend.
4. The results show a clear shift in the GS system around 2010 (Figure 8b) with high correlations between the GS flow and GS position, which may be part of a large-scale and long-term pattern (period of ~20–30 years)—this will need further research with longer records or climate models. Similar long-term cycles are seen in coastal sea level data, but the response of sea level in the SAB and the MAB are out of phase with each other. It is suggested that the closeness of the GS to the coast may be responsible for the different mechanisms operating in the SAB and the MAB.
5. The EMD analysis showed that both the GS flow and coastal sea level variability are dominated by oscillations with periods of 2–5 years. At these scales, coastal sea level is generally anticorrelated with variations in the nearby GS flow, with higher correlation coefficients in the SAB where the GS is close to the coast than in the MAB. Due to local forcing, mesoscale eddies, and recirculation gyres, at high frequencies the GS in the SAB and in the MAB have different variability and are not well correlated with each other. This result is consistent with a previous study of Ezer (2015) that found no correlation between the GS flow observed by Rossby et al. (2014) at ~38°N and the GS flow observed off the coast of Florida at 27°N (Meinen et al., 2010). Thus, a main conclusion of the study is that spatial and temporal variations along the path of the GS are closely related with spatial and temporal variations of sea level along the U.S. East Coast.

Acknowledgments
Old Dominion University's Climate Change and Sea Level Rise Initiative (CCSLRI) and the Resilience Collaborative (ODU-RC) provided partial support for this study and the Center for Coastal Physical Oceanography (CCPO) provided computational support. A. Valle-Levinson is thanked for providing useful suggestions. The hourly tide gauges sea level data are available from this site (http://opendap.co-ops.nos.noaa.gov/dods/). The Florida Current transport data are available from this site (http://www.aoml.noaa.gov/phod/floridacurrent/). The altimeter data are available from this site (http://las.aviso.oceanobs.com/ or http://marine.copernicus.eu/).

References

Baringer, M. O., & Larsen, J. C. (2001). Sixteen years of Florida current transport at 27°N. *Geophysical Research Letters*, *28*(16), 3179–3182. https://doi.org/10.1029/2001GL013246

Boon, J. D. (2012). Evidence of sea level acceleration at U.S. and Canadian tide stations, Atlantic coast, North America. *Journal of Coast Research*, *28*(6), 1437–1445. https://doi.org/10.2112/JCOASTRES-D-12-00102.1

Caesar, L., Rahmstorf, S., Robinson, A., Feulner, G., & Saba, V. (2018). Observed fingerprint of a weakening Atlantic Ocean overturning circulation. *Nature*, *556*, 191–196. https://doi.org/10.1038/s41586-018-0006-5

Chen, X., Zhang, X., Church, J. A., Watson, C. S., King, M. A., Monselesan, D., et al. (2017). The increasing rate of global mean sea-level rise during 1993–2014. *Nature Climate Change*, *7*, 492–495. https://doi.org/10.1038/nclimate3325

Domingues, R., Goni, G., Baringer, N., & Volkov, D. (2018). What caused the accelerated sea level changes along the U.S. East Coast during 2010–2015? *Geophysical Research Letters*, *45*, 13,367–13,376. https://doi.org/10.1029/2018GL081183

Ezer, T. (2013). Sea level rise, spatially uneven and temporally unsteady: Why the U.S. East Coast, the global tide gauge record, and the global altimeter data show different trends. *Geophysical Research Letters*, *40*, 5439–5444. https://doi.org/10.1002/2013GL057952

Ezer, T. (2015). Detecting changes in the transport of the Gulf Stream and the Atlantic overturning circulation from coastal sea level data: The extreme decline in 2009–2010 and estimated variations for 1935–2012. *Global and Planetary Change*, *129*, 23–36. https://doi.org/10.1016/j.gloplacha.2015.03.002

Ezer, T. (2016). Can the Gulf Stream induce coherent short-term fluctuations in sea level along the U.S. East Coast?: A modeling study. *Ocean Dynamics*, *66*(2), 207–220. https://doi.org/10.1007/s10236-016-0928-0

Ezer, T. (2017). A modeling study of the role that bottom topography plays in Gulf Stream dynamics and in influencing the tilt of mean sea level along the U.S. East Coast. *Ocean Dynamics*, *67*(5), 651–664. https://doi.org/10.1007/s10236-017-1052-5

Ezer, T. (2018). On the interaction between a hurricane, the Gulf Stream and coastal sea level. *Ocean Dynamics*, *68*, 1259–1272. https://doi.org/10.1007/s10236-018-1193-1

Ezer, T., & Atkinson, L. P. (2014). Accelerated flooding along the U.S. East Coast: On the impact of sea-level rise, tides, storms, the Gulf Stream, and the North Atlantic Oscillations. *Earth's Future*, *2*(8), 362–382. https://doi.org/10.1002/2014EF000252

Ezer, T., & Atkinson, L. P. (2017). On the predictability of high water level along the U.S. East Coast: can the Florida Current measurement be an indicator for flooding caused by remote forcing? *Ocean Dynamics*, *67*(6), 751–766. https://doi.org/10.1007/s10236-017-1057-0

Ezer, T., Atkinson, L. P., Corlett, W. B., & Blanco, J. L. (2013). Gulf Stream's induced sea level rise and variability along the U.S. mid-Atlantic coast. *Journal of Geophysical Research: Oceans*, *118*, 685–697. https://doi.org/10.1002/jgrc.20091

Ezer, T., Atkinson, L. P., & Tuleya, R. (2017). Observations and operational model simulations reveal the impact of Hurricane Matthew (2016) on the Gulf Stream and coastal sea level. *Dynamics of Atmospheres and Oceans*, *80*, 124–138. https://doi.org/10.1016/j.dynatmoce.2017.10.006

Ezer, T., & Corlett, W. B. (2012). Is sea level rise accelerating in the Chesapeake Bay? A demonstration of a novel new approach for analyzing sea level data. *Geophysical Research Letters*, *39*, L19605. https://doi.org/10.1029/2012GL053435

Goddard, P. B., Yin, J., Griffies, S. M., & Zhang, S. (2015). An extreme event of sea-level rise along the Northeast coast of North America in 2009–2010. *Nature Communications*, *6*(1), 6345. https://doi.org/10.1038/ncomms7346

Huang, N. E., Shen, Z., Long, S. R., Wu, M. C., Shih, E. H., Zheng, Q., et al. (1998). The empirical mode decomposition and the Hilbert spectrum for non stationary time series analysis. *Proceeding of the Royal Society of London*, *454*(1971), 903–995. https://doi.org/10.1098/rspa.1998.0193

Hughes, C. W., & Meredith, P. M. (2006). Coherent sea-level fluctuations along the global continental slope. *Philosphical Transections of the Royal Society*, *364*, 885–901. https://doi.org/10.1098/rsta.2006.1744

Huthnance, J. M. (1978). On coastal trapped waves: Analysis and numerical calculation by inverse iteration. *Journal of Physical Oceanography.*, *8*, 74–92. https://doi.org/10.1175/1520-0485(1978)008<0074:OCTWAA>2.0.CO;2

Joyce, T. M., Deser, C., & Spall, M. A. (2000). The relation between decadal variability of subtropical mode water and the North Atlantic oscillation. *Journal of Climate*, *13*, 2550–2569. https://doi.org/10.1175/1520-0442(2000)013

Kenigson, J. S., & Han, W. (2014). Detecting and understanding the accelerated sea-level rise along the east coast of United States during recent decades. *Journal of Geophysical Research: Oceans*, *119*, 8749–8766. https://doi.org/10.1002/2014JC010305

McCarthy, G., Frejka-Williams, E., Johns, W. E., Baringer, M. O., Meinen, C. S., Bryden, H. L., et al. (2012). Observed interannual variability of the Atlantic Meridional Overturning Circulation at 26.5°N. *Geophysical Research Letters*, *39*, L19609. https://doi.org/10.1029/2012GL052933

Meinen, C. S., Baringer, M. O., & Garcia, R. F. (2010). Florida current transport variability: An analysis of annual and longer-period signals. *Deep Sea Research*, *57*(7), 835–846. https://doi.org/10.1016/j.dsr.2010.04.001

Park, J., & Sweet, W. (2015). Accelerated sea level rise and Florida current transport. *Ocean Science*, *11*, 607–615. https://doi.org/10.5194/os-11-607-2015

Piecuch, C. G., Dangendorf, S., Ponte, R., & Marcos, M. (2016). Annual sea level changes on the North American Northeast Coast: influence of local winds and barotropic motions. *Journal of Climate*, *29*, 4801–4816. https://doi.org/10.1175/JCLI-D-16-0048.1

Piecuch, C. G., & Ponte, R. M. (2015). Inverted barometer contributions to recent sea level changes along the northeast coast of North America. *Geophysical Research Letters*, *42*, 5918–5925. https://doi.org/10.1002/2015GL064580

Rossby, T., Flagg, C. N., Donohue, K., Sanchez-Franks, A., & Lillibridge, J. (2014). On the long-term stability of Gulf Stream transport based on 20 years of direct measurements. *Geophysical Research Letters*, *41*, 114–120. https://doi.org/10.1002/2013GL058636

Sallenger, A. H., Doran, K. S., & Howd, P. (2012). Hotspot of accelerated sea-level rise on the Atlantic coast of North America. *Nature Climate Change*, *2*, 884–888. https://doi.org/10.1038/NCILMATE1597

Smeed, D. A., McCarthy, G., Cunningham, S. A., Frajka-Williams, E., Rayner, D., Johns, W. E., et al. (2013). Observed decline of the Atlantic Meridional Overturning Circulation 2004 to 2012. *Ocean Science*, *10*, 29–38. https://doi.org/10.5194/osd-10-1619-2013

Sweet, W., & Park, J. (2014). From the extreme to the mean: Acceleration and tipping points of coastal inundation from sea level rise. *Earth's Future*, *2*(12), 579–600. https://doi.org/10.1002/2014EF000272

Valle-Levinson, A., Dutton, A., & Martin, J. B. (2017). Spatial and temporal variability of sea level rise hot spots over the eastern United States. *Geophysical Research Letters*, *44*, 7876–7882. https://doi.org/10.1002/2017GL073926

Wdowinski, S., Bray, R., Kirtman, B. P., & Wu, Z. (2016). Increasing flooding hazard in coastal communities due to rising sea level: Case study of Miami Beach, Florida. *Ocean Coastal Management*, *126*, 1–8. https://doi.org/10.1016/j.ocecoaman.2016.03.002

Woodworth, P. L., Maqueda, M. M., Gehrels, W. R., Roussenov, V. M., Williams, R. G., & Hughes, C. W. (2016). Variations in the difference between mean sea level measured either side of Cape Hatteras and their relation to the North Atlantic Oscillation. *Climate Dynamics*, *49*(7-8), 2451–2469. https://doi.org/10.1007/s00382-016-3464-1

Wu, Z., & Huang, N. (2009). Ensemble Empirical Mode Decomposition: A noise-assisted data analysis method. *Advances in Adaptive Data Analysis*, *01*(01), 1–41. https://doi.org/10.1142/S1793536909000047

Yin, J., & Goddard, P. B. (2013). Oceanic control of sea level rise patterns along the East Coast of the United States. *Geophysical Research Letters*, *40*, 5514–5520. https://doi.org/10.1002/2013GL057992